

TWO MODE - (DE)MUXER BASED ON A SYMMETRIC Y JUNCTION COUPLER, A 2×2 MMI COUPLER AND A RIDGE PHASE SHIFTER USING SILICON WAVEGUIDES FOR WDM APPLICATIONS

DUNG CAO TRUONG^{1,†}, DAO ANH VU² AND CHUNG VU HOANG²

¹*Posts and Telecommunications Institute of Technology, Hanoi, Vietnam*

²*Institute of Materials Science, Vietnam Academy of Science and Technology, Hanoi, Vietnam*

[†]*E-mail: dungtc@ptit.edu.vn*

Received 13 November 2017

Accepted for publication 11 December 2017

Published 31 December 2017

Abstract. *In this paper, we introduce a new two-mode (de)multiplexer based on the silicon-on-insulator (SOI) platform. The device is built on a symmetric Y-junction, a 2×2 multimode interference (MMI) waveguide and a phaseshifter in the form of a ridge waveguide which is designed using 3D scalar beam propagation method (BPM). The phase evolution in the structure is discussed in details. The simulation results show that the device can operate in a wide wavelength range (150 nm) with a low insertion loss and small crosstalk. A large fabrication tolerance to the width of the input waveguide up to 100 nm is achieved, which is compatible to the current CMOS manufacturing technologies for the photonic integrated circuits. Furthermore, the small footprint ($4 \mu\text{m} \times 286 \mu\text{m}$) makes the device suitable for applications in high bitrate and compact on-chip silicon photonic integrated circuits.*

Keywords: two-mode (de)multiplexer, symmetric Y-junction, MMI coupler, silicon on insulator (SOI), beam propagation method (BPM), effective index method (EIM).

Classification numbers: 42.65.Wi; 42.82.Et; 42.65.Hw.

I. INTRODUCTION

In the era of the rapid growth of bandwidth demands in the information networks for video on demand, cloud computing and big data, communication systems relied on the wavelength-division multiplexing (WDM) technology [1] are now approaching the limitation of Shannon's information theory limit [2] and the nonlinear effects in optical fiber [3]. The data transmission capacity in each wavelength can be improved by using advanced techniques such as space division multiplexing (SDM), polarization division multiplexing (PDM) [4], and higher order modulation formats [5, 6]. The SDM [7] has recently been proposed as a potential technology to keep up the demands in traffic growth in optical transmission systems. In the SDM method, spatially separated channels are used to propagate multiple signals. Multimode division multiplexing (MDM) has been also demonstrated in multi-core fibers [8] or few-mode fibers (FMF) [9–13]. SDM has drawn much attention thanks to its advantages namely cost-effective, dedicated space and energy saving. The PDM is also another promising method to increase the capacity but this method requires additional separate polarization states individually, this make PDM become more suitable for dual polarization modulation formats. Otherwise, higher order modulation formats [5] give an enhancement of the capacity by mean of increasing spectrum efficiency but they suffered from the decrease of the transmission distance. Recently, mode-division multiplexing (MDM) [14, 15] has emerged as an efficient approach to further increase the transmission capability. In the MDM method, each optical mode is considered as an independent channel for carrying optical signal. It is seen clearly that a tremendous increase in transmission capacity can be realized by combining MDM with WDM, PDM, and multi-level modulation. A significant advantage of MDM is to sustain nonlinearity of the optical fiber and orthogonality of waveguide modes in order to eliminating the intermodal interference.

Recently, the combination between WDM and MDM communication systems has been demonstrated as a key to enhance the transmission capacity of photonic devices. Particularly, planar lightwave circuit (PLC)-based MDM devices using silicon on insulator (SOI) material platform has some remarkable advantages of high flexibility, relatively low loss, high confinement of light due to high core-cladding (Si/SiO₂) refractive index difference and high compactness, mass-production due to their mature fabricating technology [16]. A compact and reconfigurable mode (de)multiplexer which can support numerous modes is essential for realizing the MDM-WDM in integrated photonics [17].

Some designs of MDMs have been proposed based on multi-mode interference (MMI) couplers [18–21] which typically exhibit advantages such as broadband, large tolerance fabrications. Others based on asymmetric directional couplers [22, 23] and Y-junctions [24, 25] have relative complexity for the manufacture and quite large insertion loss. Similarly, several three mode (de)multiplexers using adiabatic asymmetric resonators [26] to realize reconfigurable (de)multiplexing functions. However those structures have a narrow resonant bandwidth.

In this paper, we propose a new-structure of the two-mode on chip (de)multiplexer (TM-(de)MUXer) which is constructed in a form of a compact symmetric Y-junction coupler, a 2×2 MMI coupler and a ridge phase shifter using silicon material. We investigate the operation of this device numerically by mean of scalar beam propagation method (BPM). We show that this device is compact, low loss, ultra-broadband, and relatively large fabrication tolerances, which are suitable for applications on high data rate integrated photonic circuits.

II. DESIGN PRINCIPLE AND STRUCTURE OPTIMIZATION

Figure 1 shows the schematic structure of the proposed TM-(de)MUXer. At the input, a symmetric Y-junction coupler is used to divide the fundamental mode and the first order mode similarly to a 3-dB coupler. Then, a 2×2 MMI coupler with a phase shifter (PS) that is formed a ridge waveguide inserted at one of the input ports to separate two optical paths into two output ports individually. The waveguides are made of the silicon layer that is embedded on a silica layer with the upper cladding of air. Refractive indices of the layers are: the silicon core layer $n_r = 3.457$, the silica cladding layer $n_c = 1.444$, the air $n_{air} = 1$. The device is designed in the three-dimensional space waveguides, operating in 1550 nm wavelength range. Silicon waveguides are proposed to be fabricated in the form of standard silicon on insulator (SOI) wafer with the total height $H = 220$ nm and the slab height $h_0 = 130$ nm, respectively. The device can be fabricated with the E-beam lithography and etched down to the substrate layer by using inductively coupled plasma etching technique with a photoresist layer, such as Poly(methyl methacrylate) (PMMA). Cladding silica layer is created by using plasma-enhanced chemical vapor deposition (PECVD) method.

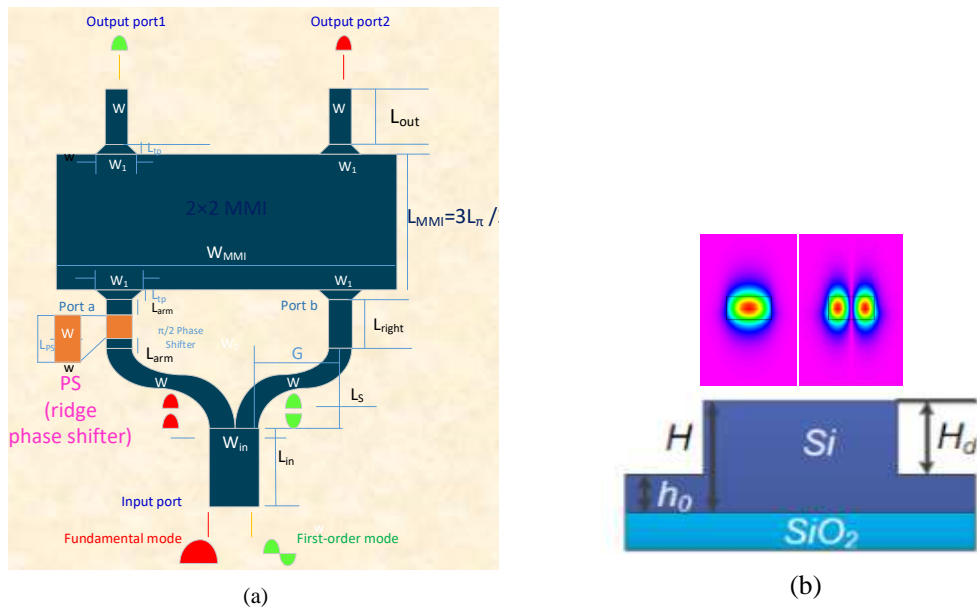


Fig. 1. (a) Schematic of the proposed TM-(de)MUXer and (b) the structure of silicon ridge waveguide.

Firstly, we use the symmetric Y-junction coupler to divide equally the fundamental mode and the first order mode in the polarization state of TE. The Y-junction coupler composes of a stem at the input port is a straight waveguide whose width is W_{in} . The stem waveguide only supports for the operation of two order modes. The output ports of the Y-junction coupler consists of two S-bent waveguides placed symmetrically. S-bent waveguides have the length in the propagation direction as L_s and the distance in the transverse directional as G chosen previously as $1.6 \mu\text{m}$. The width of S-bent is chosen as 500 nm for satisfying the single mode condition of the wavelength

1550 nm [27]. EIM method incorporated with scalar BPM method are utilized for simulation the width of the Y-junction coupler stem W_{in} , aiming to find out the condition so that the Y-junction coupler only support for the operation of the fundamental mode and the first order mode. To save the simulation time but still ensure an essential accuracy for simulation, in whole this design we use a 3D-scalar BPM simulation with grid sizes as follows: $\Delta x = \Delta y = \Delta z = 20$ nm (we found that the smaller grid size does not affect significantly the simulation results). Without the polarity of guided modes, the 3D scalar BPM is utilized to accurately approximate for numerical solutions of the guided mode in the optical waveguide [28]. It is seen in Fig. 2, simulation results by BPM method for effective indices of the Y-junction stem show that the cutoff-condition for limiting two guided modes in the Y coupler has been occurred at the width $W_{in} \leq 1.2 \mu\text{m}$. Therefore, in this design, we choose the width of the Y-junction stem as $W_{in} = 1.2 \mu\text{m}$. We use the Y-junction coupler to divide two guided modes similarly to the idea from Love *et al.* [25] but using S-bent waveguides at the output of the Y-junction coupler instead of using straight waveguides because the S-bent waveguides is less loss at the joint at the Y-junction coupler output than the straight ones. The BPM simulation has also showed that the optimal length of S-bent for the best performance of divided transmission property of two guided modes is chosen at the length of $L_s = 80 \mu\text{m}$ (therefore, the bent radius of S-bent waveguides is $1231 \mu\text{m}$). In Fig. 1, the red parts denote the fundamental mode and the green ones stand for the first-order mode (as seen in Fig. 1).

In the next section, we use the 2×2 MMI coupler to realize the function of (de)multiplexing for two guided modes. The 2×2 MMI coupler based on general interference (GI) mechanism. Two output branches of the symmetric Y-junction coupler is connected to two access waveguides of the MMI coupler by straight waveguides in the propagation direction that only operated in single mode mechanism. It is well-known that the symmetric Y-junction coupler can divide the fundamental mode with two balanced-power and in-phase outputs while dividing the first order mode with two balanced-power and counter-phase outputs.

Aiming to make the optical combination, the 2×2 MMI coupler is designed as a shortest possible 3-dB coupler. Two access waveguides are connected to the outputs of the MMI coupler.

Hence, in this proposed design, we choose the width of the MMI coupler as $W_{MMI} = 4 \mu\text{m}$. In the GI mechanism, the half beat-length L_π of the MMI coupler is defined as [29]:

$$L_\pi = \frac{4n_e W_{eff}^2}{3\lambda} \quad (1)$$

Here, W_{eff} is the effective width of the multimode region, it is defined in TE polarization state as follow:

$$W_{eff} = W_{MMI} + \frac{\lambda}{\pi} (n_e^2 - n_c^2)^{-1/2} \quad (2)$$

where n_e and n_c are denoted to the effective refractive index of the core layer and refractive index of the cladding layer, respectively; λ is the wavelength in the free space. The MMI coupler operate as the 3dB-coupler at the shortest length of the MMI region is defined by the relation: $L_{MMI} = 3L_\pi/2$. Using the result of effective index, we obtain the shortest length L_{MMI} to be $\sim 67 \mu\text{m}$ by the theory of mode propagation method. Because the calculation by using mode propagation analysis (MPA) method is an approximation, we therefore continue to use the BPM simulation for the length of the MMI region around the MPA method. As result, the optimal length of the MMI region has been chosen equally $65 \mu\text{m}$. At this length, the transfer matrix of the MMI coupler can easily obtain

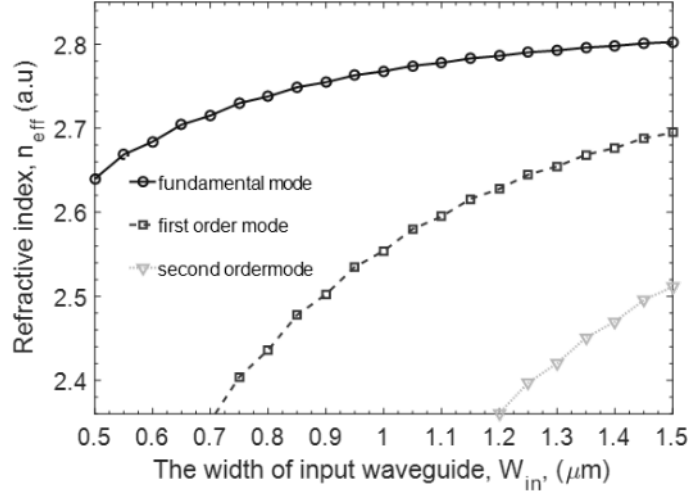


Fig. 2. Effective index of the stem of the symmetric Y-junction coupler as a function of the waveguide width.

from Bachmann *et al.* [30] expressed as:

$$M = \frac{1}{\sqrt{2}} \begin{pmatrix} 1 & j \\ j & 1 \end{pmatrix} \quad (3)$$

If we represent the amplitude of the optical fields in the matrix relation, transfer matrices of guided modes at output ports of the Y-junction coupler can be expressed for the fundamental mode, the first mode as follows:

$$Y_0 = \frac{1}{\sqrt{2}} \begin{pmatrix} e^{j\pi/2} \\ e^{j\pi/2} \end{pmatrix} e^{j\theta_0}, \quad Y_1 = \frac{1}{\sqrt{2}} \begin{pmatrix} e^{j\pi/2} \\ e^{-j\pi/2} \end{pmatrix} e^{j\theta_1} \quad (4)$$

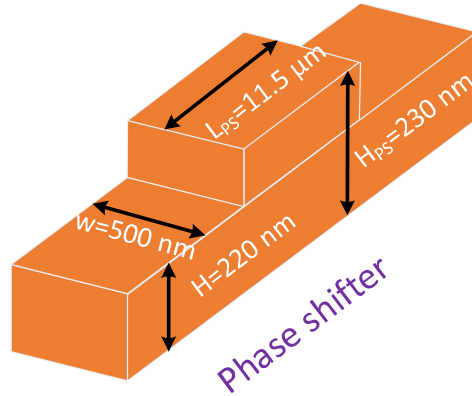
where θ_0 and θ_1 are accumulated initial phase angles by the fundamental mode and the first order mode, respectively.

To achieve the function of multiplexing (or demultiplexing) by combining two optical paths at two input ports of the 2×2 MMI coupler, a phase shifter (PS) is placed at one arm of the input ports. Without loss of generality, we assume that the PS is placed onto the left arm between at the Y-junction coupler and the MMI coupler, as can be seen in Fig. 1. Guided wave propagation for two guided modes at the outputs of the MMI coupler when shifting a phase angle Φ are expressed consecutively by the transfer matrix method as follows:

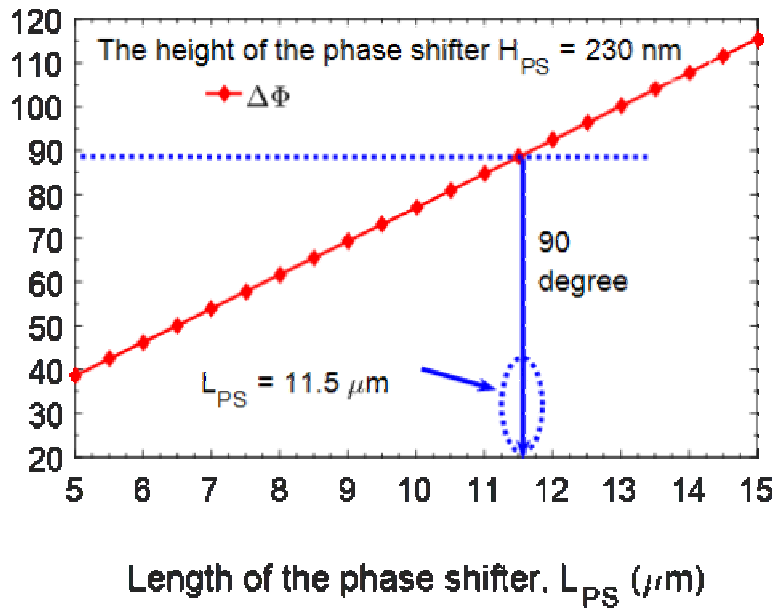
$$\begin{aligned} X_0 &= MY_0 = \frac{1}{2} \begin{pmatrix} 1 & j \\ j & 1 \end{pmatrix} \begin{pmatrix} e^{j(\pi/2+\Phi)} \\ e^{j\pi/2} \end{pmatrix} e^{j\theta_0}, \\ X_1 &= MY_1 = \frac{1}{2} \begin{pmatrix} 1 & j \\ j & 1 \end{pmatrix} \begin{pmatrix} e^{j(\pi/2+\Phi)} \\ e^{-j\pi/2} \end{pmatrix} e^{j\theta_1} \end{aligned} \quad (5)$$

It is easy to examine that the phase shift angle $\Phi = \pm\pi/2$ satisfies the (de)multiplexing condition in equation system (5). The fundamental mode will be combined to the output 2 of

the MMI coupler and the first order mode will lead to the output 1 of as can be indicated by symbols as the red one and the gold one in Fig. 1.



(a)



(b)

Fig. 3. Phase difference of the phase shifter (PS) as a function of the length L_{PS} .

In this paper, we design the PS in the form of a ridge waveguide structure [31] (see the zoomed part in Fig. 1(a) and the extracted part in Fig. 3(a)). When the ridge height of the PS becomes broader or smaller, the effective index become bigger or smaller (see Fig. 3), which

equals providing the upper waveguide with the earlier line or delay line. Thus, the PS makes phase difference between the lights through the PS and the same long straight waveguide. The phase shift angle for the light propagating through the PS can be calculated theoretically by following expression:

$$\Phi(0, L_{PS}) = \int_0^{L_{PS}} (\beta_0(z) - \beta_{PS}(z)) dz \quad (6)$$

where L_{PS} is the length of the PS, $\beta_0(z)$ and $\beta_{PS}(z)$ denote the propagation constants of the fundamental mode in straight waveguide and the *PS* waveguide, respectively; n_e is the effective index of the core layer.

In this design, we choose the height of the PS to be $H_{PS} = 230$ nm (a 10 nm-thick layer is covered on the left arm of the Y-coupler, as seen in Fig. 3(a)). The BPM simulation is used to investigate the dependence of the phase shift angle Φ as a function of the length L_{PS} of the *PS*. As can be seen in Fig. 3(b), the phase difference between the PS for the operation wavelength of 1550 nm at the left arm in comparison with the straight waveguide at the right arm achieve equally 90 degree ($\pi/2$ radian) at the length the PS as $L_{PS} = 11.5$ μm (as seen in the marked point of Fig. 3(b)).

III. PERFORMANCE EVALUATION AND DISCUSSION

Figures 4(a) and (b) show the field distributions of the mode (de)MUXer at the operation wavelength of 1550 nm when input ports are launched discretely (the fundamental mode and first-order mode of scalar optical fields, respectively). It can be seen that the light is efficiently propagated into the proposed structure and there is a little power radiated out of the guided-wave regions.

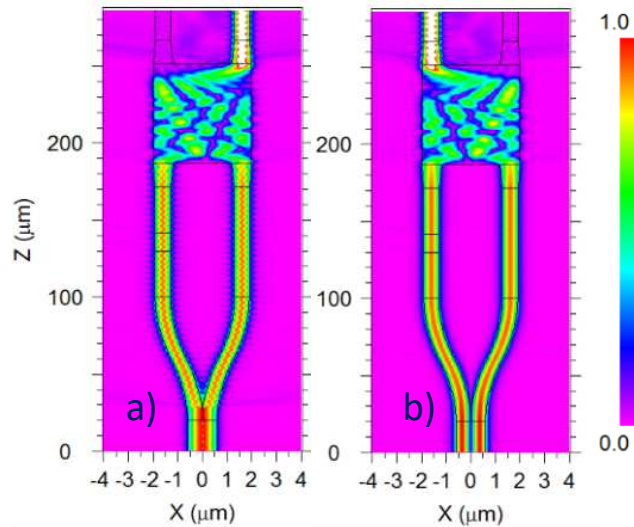


Fig. 4. Electric field distribution for the proposed TM- (de)MUXer: the fundamental mode is launched a), the first order mode is launched b).

For a mode (de)multiplexer, most important factors are insertion loss (I.L) and crosstalk (Cr.T) which are defined as following:

$$I.L = 10 \log_{10} \left(\frac{P_{out}}{P_{in}} \right) \quad (7)$$

$$Cr.T = -10 \log_{10} \left(\frac{P_{out}}{P_{unwanted}} \right) \quad (8)$$

where P_{in} is the input power of the device, P_{out} and $P_{unwanted}$ are the wanted and unwanted output powers of the device, respectively. Simulation results obviously show that the proposed device has a low insertion loss and crosstalk.

Optical bandwidth is a very important parameter for mode (de)multiplexer. Fig. 5 shows the wavelength dependence of the insertion loss and crosstalk for the fundamental mode and the first order mode as the wavelength varies from 1500 nm to 1650 nm, covering the whole C and L bands. The input power is normalized equally 1 power unit. It can be seen that the proposed device has a low insertion loss and low crosstalk in which the insertion loss varies from 0.5 dB to 1 dB and the crosstalk is below -25 dB in the bandwidth of 150 nm, as can be seen in Fig. 5.

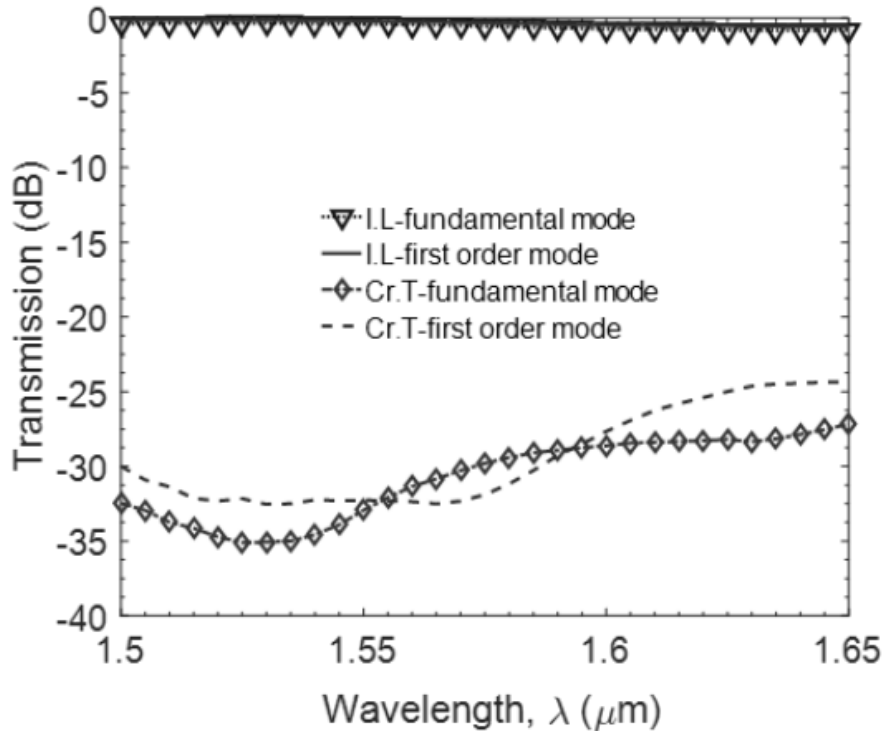


Fig. 5. Wavelength dependency of the proposed TM-(de)MUXer in the 150 nm bandwidth.

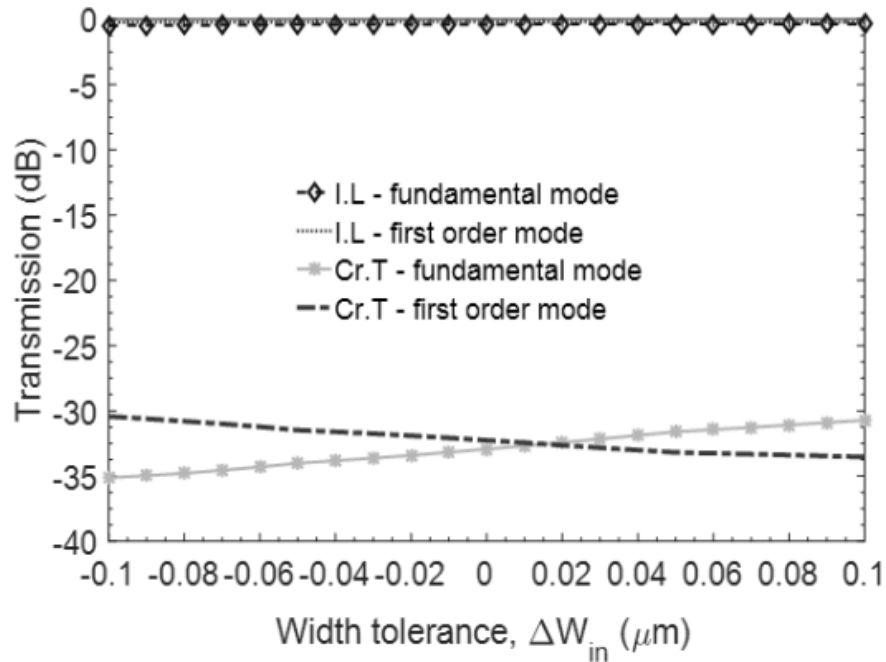


Fig. 6. Transmission of the proposed device as a function of the width tolerance of the input port waveguide W_{in} .

Fabrication tolerance is of importance for the operation of an optical waveguide-based device. It is well-known that the MMI coupler has a large tolerance compared with its size parameter variations [32, 33]. In this design, we investigate the influence of other crucial geometrical tolerances to the optical performance of the proposed device. Firstly, we survey the width tolerance of the input waveguide. The BPM simulation results presented in Fig. 6 show that the insertion loss is about 0.8 dB and crosstalk is kept below -30 dB as ΔW_{in} varies in the range up to ± 100 nm. Secondly, the S-bent length L_s has an important impact to the branching angles of the Y-junction coupler. Thus, we consider the variation of the S-bent length on to the operation of the device. Fig. 7 plots the transmission of the device as a function of the length tolerance of the Y-junction coupler. We can see that, the insertion loss stays nearly the same and fundamental mode of the crosstalk changes slightly in a tolerance of ± 10 μm of the S-bent length tolerance. Finally, we study the tolerance of the total height of the ridge waveguides. As the thickness of a SOI wafer cannot be controlled during the fabrication, therefore it depends on the quality of the supplied samples. The height tolerance (the thickness of the SOI wafer) of ridge waveguides is presented as seen in Fig. 8 by the BPM simulation. Simulation data shows that a small variation of ± 2 nm in the thickness of the SOI wafer induces a rather large change at the crosstalk. However, the crosstalk change is kept below -15 dB and the insertion loss is smaller than 1 dB. The 2nm-accuracy can be achieved by using the current CMOS technology (excimer laser photolithography, also known as 193 nm DUV photolithography) for the fabricating of the silicon photonic integrated circuits.

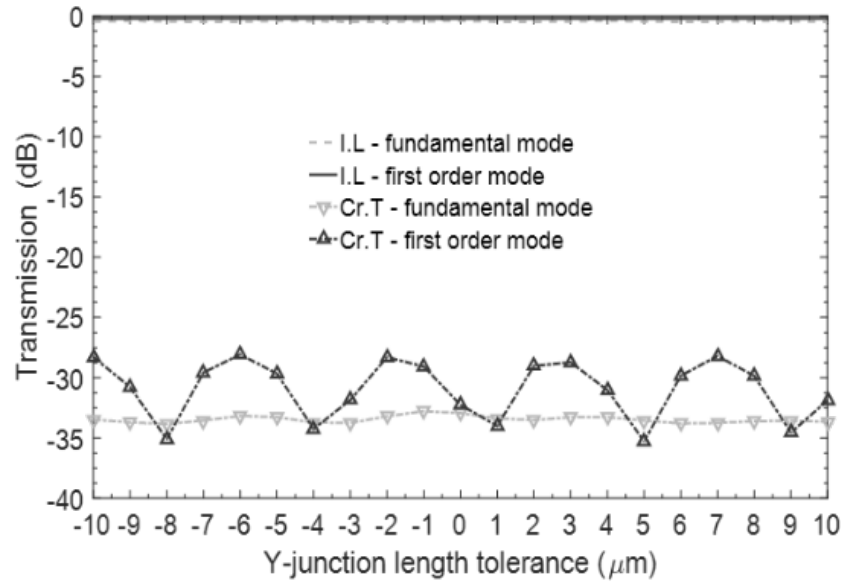


Fig. 7. Transmission of the proposed device as a function of the length tolerance of the Y-junction coupler.

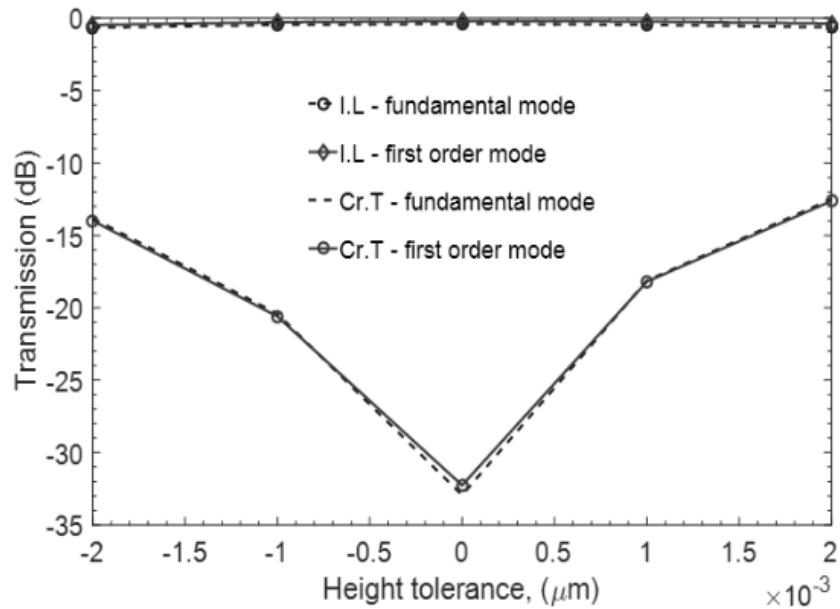


Fig. 8. Transmission of the proposed device as a function of the height tolerance of ridge waveguides.

IV. CONCLUSIONS

We have presented a numerical simulation design of a high-performance TM-(de)MUXer which is based on the symmetric Y-junction coupler and a 2×2 MMI coupler using the silicon on insulator (silica) material platform. A scalability of the proposed design can be created, for instance, a structure of three-mode (de)MUXer can be achieved by mean of a trident – junction coupler instead of the Y-junction coupler. Obtained results show a successful operation of a two-mode (de)multiplexer for the fundamental mode and the first order mode. The performance analysis for the proposed device is carried out by using 3D-scalar BPM simulation. The results have shown that the device has a low insertion loss and crosstalk. These features make the device a very promising candidate for the MDM-WDM systems. Furthermore, since the whole size of the proposed device can be integrated on a footprint as $4 \mu\text{m} \times 286 \mu\text{m}$, it is potentially suitable for applications on high-speed on-chip photonics integrated circuits.

ACKNOWLEDGMENT

This research is funded by Ministry of Information and Communication of Vietnam under the grant program for the contract number T.025/17 in the year of 2017.

REFERENCES

- [1] N. S. Bergano and C. R. Davidson, *J. Light. Technol.* **14** (1996) 1299.
- [2] R. Essiambre et al., *J. Light. Technol.* **28** (2010) 662.
- [3] A. D. Ellis, J. Zhao, and D. Cotter, *J. Light. Technol.* **28** (4) (2010) 423.
- [4] S. L. Jansen, I. Morita, T. C. W. Schenk, and H. Tanaka, *J. Opt. Netw.* **7** (2008) 173.
- [5] N. Bozinovic et al., *Science*. **340** (6140) (2013) 1545.
- [6] R. W. Tkach, *Bell Labs Tech. J.* **14** (2010) 3.
- [7] D. J. Richardson, J. M. Fini, and L. E. Nelson, *Nat. Photonics*. **7** (2013) 354.
- [8] H. Kubota, M. Oguma, and H. Takara, *IEICE Electron. Express*. **10** (12) (2013) 1.
- [9] S. G. Leon-Saval, N. K. Fontaine, J. R. Salazar-Gil, B. Ercan, R. Ryf, and J. Bland-Hawthorn, *Opt. Express* **22** (2014) 1036.
- [10] R. Ryf et al., *J. Light. Technol.* **30** (2012) 521.
- [11] S. Randel et al., *Opt. Express*. **19** (2011) 16697–16707.
- [12] M. Salsi et al., *J. Light. Technol.* **30** (2012) 618.
- [13] N. Bai et al., *Opt. Express*. **20** (2012) 2668.
- [14] F. Saitoh, K. Saitoh, and M. Koshiba, *Opt. Express*. **18** (2010) 4709.
- [15] B. A. Dorin and W. N. Ye, in *OFC International Conf.* (2014) 4–6.
- [16] N. Hanzawa et al., *Opt. Express*. **22** (24) (2014) 29321–29330.
- [17] A. M. J. Koonen, H. Chen, H. P. A. Van Den Boom, and O. Raz, *IEEE Photonics Technol. Lett.* **24** (2012) 1961.
- [18] Y. Huang, G. Xu, and S. T. Ho, *IEEE Photonics Technol. Lett.* **18** (2006) 2281.
- [19] T. Uematsu, Y. Ishizaka, Y. Kawaguchi, K. Saitoh, and M. Koshiba, *J. Light. Technol.* **30** (2012) 2421.
- [20] S. Bagheri and W. M. J. Green, in *6th IEEE International Conference on Group IV Photonics* (2009) 166.
- [21] L. Han, S. Liang, H. Zhu, L. Qiao, J. Xu, and W. Wang, *Opt. Lett.* **40** (2015) 518.
- [22] J. B. Driscoll, R. R. Grote, B. Souhan, J. I. Dadap, M. Lu, and R. M. Osgood, *Opt. Lett.* **38** (2013) 1854.
- [23] Y. De Yang, Y. Li, Y. Z. Huang, and A. W. Poon, *Opt. Express*. **22** (2014) 22172.
- [24] Y. Li, C. Li, C. Li, B. Cheng, and C. Xue, *Opt. Express*. **22** (2014) 5781.
- [25] J. D. Love, N. Riesen, *J. Light. Technol.* **30** (2012) 304.
- [26] L.-W. Luo et al., *Nat. Commun.* **5** (3069) (2014) 1.
- [27] S. T. Lim, C. E. Png, E. A. Ong, and Y. L. Ang, *Opt. Express*. **15** (2007) 11061.
- [28] A. Ortega-Monux, I. Molina-Fernandez, and J. G. Wanguemert-Perez, *Opt. Quantum Electron.* **37** (2005) 213.

- [29] L. B. Soldano and E. C. M. Pennings, *J. Light. Technol.* **13** (1995) 615.
- [30] M. Bachmann, P. A. Besse, and H. Melchior, *Appl. Opt.* **33** (1994) 3905.
- [31] S. H. Jeong and K. Morito, *J. Light. Technol.* **28** (2010) 1323.
- [32] P. A. Besse, M. Bachmann, H. Melchior, L. B. Soldano, and M. K. Smit, *J. Light. Technol.* **12** (1994) 1004.
- [33] C. D. Truong, D. H. Tran, T. A. Tran, and T. T. Le, *Opt. Commun.* **292** (2013) 78.